Smart Materials

DOI: 10.1002/anie.201204139

A Smart Nanofiber Web That Captures and Releases Cells**

*Young-Jin Kim, Mitsuhiro Ebara, and Takao Aoyagi**

Nanofiber webs are finding an ever-increasing range of applications, including as filter fabrics,[1] sensors,[2] and electronic devices,[3] as well as medical/pharmaceutical[4] applications. One new class of nanofiber webs with considerable potential for use in these rapidly growing fields are "smart" nanofiber webs, which are fabricated from stimuli-responsive polymers.[5] Nanoscale structures inherent to stimuli-responsive polymers enable highly sensitive responses to external stimuli, and the incorporation of stimuli-responsive polymers into nanofibers takes advantage of the extremely large surface area and porosity of nanofibers to generate a precision "on-off" switch to control the morphology and function of the nanofiber.[6] Extension of these nanoscale effects to the macroscale enables manipulation of the bulk matter and creates the opportunity to develop profitable new applications. Herein, we report the synthesis and application of photo-cross-linkable temperature-responsive polymer-based nanofiber webs with dynamically and reversibly tunable web properties, including swelling/shrinking, mechanical strength, and porosity. We demonstrate the ability to capture, encapsulate, and release cells by dynamically transforming the fibrous structure of the nanofibers into hydrogel-like structures by wrapping, swelling, and deswelling processes in response to alternations of external temperature (Figure 1 a). This novel nanofiber enables the facile encapsulation and on-demand release of cells in response to external signals.

Electrospinning has gained popularity in the last decade because it is a versatile and cost-effective method for the fabrication of nonwoven nanofibers with nanoscale properties.[7] Electrospinning is applicable to almost any soluble or fusible polymer and allows for the production of a variety of continuous fibers with uniform diameters that range from the micro- to the nanometer scale.[8] Recently, multifunctional

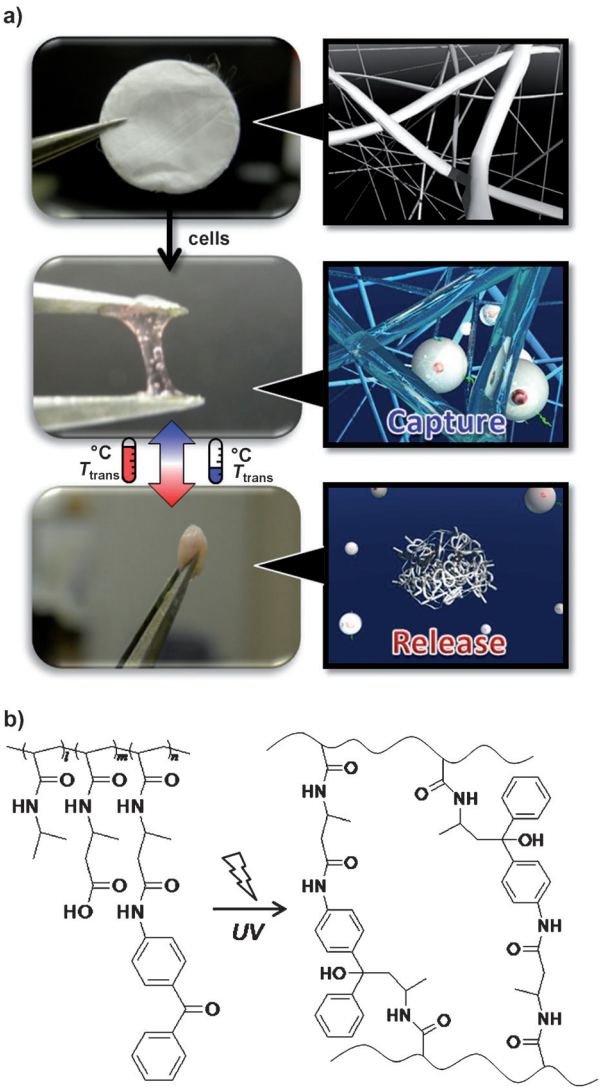

Figure 1. a) Facile capture and release of cells by using a nanofiber web that transforms from a fibrous to a hydrogel-like structure by wrapping, swelling, and shrinking processes in response to temperature changes. b) Photo-cross-linking of a newly synthesized temperature-responsive polymer.

nanofibers were successfully developed by electrospinning polymers blended with additional compound such as carbon nanotubes,[9] ceramics,[10] and biomolecules,[11] or by surface modification[12] with peptides or proteins. These functional nanofibers are promising for more diverse applications such as in drug-delivery systems,[13] tissue engineering scaffolds,[14] and wound healing.[15] In addition, the development of "smart" nanofibers that have the ability to trigger or turn material properties "on" or "off" in response to external stimuli is critically important for the control of biological

[*] Y.-J. Kim, Prof. T. Aoyagi
Materials and Science Engineering, Graduate School of Pure and Applied Science, University of Tsukuba
1-1-1 Tennodai, Tsukuba, Ibaraki 305-8577 (Japan)
E-mail: aoyagi.takao@nims.go.jp
Y.-J. Kim, Dr. M. Ebara, Prof. T. Aoyagi
Biomaterials Unit, International Center for Materials Nanoarchitectonics (WPI-MANA)
National Institute for Materials Science (NIMS)
1-1 Namiki, Tsukuba, Ibaraki 305-0044 (Japan)

[**] We would like to express our gratitude to the Grants-in-Aid for Young Scientists (A) (10013481) from the Ministry of Education, Culture, Sports, Science, and Technology (MEXT) Japan. We are grateful to Prof. Allan S. Hoffman (University of Washington) and Dr. John M. Hoffman (Stratos Genomics Inc. in USA) for continued and valuable discussion.

Supporting information for this article is available on the WWW under http://dx.doi.org/10.1002/anie.201204139.

activities for biotechnological[16] and biomedical[17] applications. Therapeutic cell delivery is an example of such an application, and in situ gelation[18] as well as hydrogel-based vehicles[19] are being increasingly employed. Most problems, however, lie with the reagents and the by-products of cross-linked hydrogels, which have the potential to be toxic to cells.[20] Increased cell death has been observed with a high concentration of exposed unreacted side chains after gelation.[21] Moreover, release of the encapsulated cells from vehicles is a difficult, potentially harmful process.[22] Smart nanofiber webs have the potential to be used for the facile encapsulation and on-demand release of cells in response to temperature stimulus, and thus they have promising applications for cell manipulation. One of the major challenges in the development of "smart" nanofiber webs is the design of nanofibers with dynamically and reversibly tunable web structures on both the nano- and macroscopic scale. This was achieved by electrospun copolymers of *N*-isopropylacrylamide (NIPAAm) with a UV-reactive benzophenone (BP) conjugated co-monomer (Figure 1 b). The NIPAAm homopolymer is one of the most studied temperature-responsive polymers, which undergoes a sharp transition from a hydrophilic state to a hydrophobic state at the lower critical solution temperature (LCST).[23] However, as a result of the solubility of the NIPAAm homopolymer in aqueous solutions below the LCST, the resulting nanofiber is not stable in water and readily disperses.[24] Therefore, chemical cross-linking with BP was employed (Figure 1 b). 2-Carboxyisopropylacrylamide (CIPAAm) was chosen for BP conjugation because the copolymerization of NIPAAm with carboxy-containing co-monomers such as acrylic acid (AAc) eliminates the LCST behavior of the copolymer.[25] Indeed, the use of CIPAAm, which has a similar structure to NIPAAm, has proven to result in a sharp phase transition.[26] Moreover, it has been shown that the sequence of monomers in NIPAAm and CIPAAm copolymers is completely random and that the polymer composition is the same as the co-monomer feed since the reactivity ratios for NIPAAm and CIPAAm are very similar[27] (see Table S1 in the Supporting Information). All the copolymers have a molecular weight of approximately 20 kDa. Successful conjugation of BP was confirmed by ^{1}H NMR spectroscopy. 0, 1.0, and 2.0 mol% BP was introduced into the copolymers with 1.0, 3.0, and 5.0 mol% CIPAAm in the feed (BP0, BP1, and BP2), respectively. The effect of the CIPAAm content on the LCST in pH 7.4 phosphate buffered saline (PBS) before and after BP conjugation was investigated (see Figure S1 in the Supporting Information). Before conjugation of the BP, the LCST gradually rises as the CIPAAm content increases, while it decreases after the conjugation because of the hydrophobic nature of BP.

Electrospinning is an interdisciplinary process which requires sufficient knowledge of polymer chemistry, fluid mechanics, and electrohydrodynamics.[28] Therefore, it is essential to determine appropriate values for the viscosity, flow rate, and electric field strength to produce nanoscale fibers. In particular, the viscosity, which is determined by the solution concentration, has a dominant effect on the jet behavior.[29] Therefore, a higher molecular weight (>100 kDa) is required to produce nanofibers, particularly for water-soluble acrylamide-type polymers. In this study, however, all the copolymers have relatively low molecular weights (approximately 20 kDa) in regards to producing continuous and smooth fibers by electrospinning. Therefore, a simple free-radical polymerization was used to obtain copolymers with a relatively large molecular weight distribution that could help in the entanglement of polymer chains in the nanofibers, thus making them more stable. When the concentration was lower than 10 w/v%, electrospinning resulted in beaded fibers, a process called electrospraying. Increasing the concentration above 12 w/v%, on the other hand, resulted in the formation of microscale fibers. Given these caveats, we optimized the parameters of electrospinning as follows: The copolymer was first dissolved in 1,1,1,3,3,3-hexafluoro-2-propanol (HFIP) at 11 w/v% and then subjected to voltages of 15 kV. The electrospun nanofibers were subsequently exposed to UV illumination to form cross-linked webs (the SEM images of electrospun nanofibers before and after irradiation with UV light for 30 min are shown in Figure S2 in the Supporting Information). The nanofibers were randomly distributed to form the continuous and smooth fibrous web with a diameter of predominately 600–800 nm. It can also be seen that the fibers preserve their morphology even after illumination with UV light (for the fiber diameter distribution of BP2 see Figure S3 in the Supporting Information). Irradiation with UV light and subsequent cross-linking did not alter this distribution.

The photo-cross-linking of the electrospun nanofiber webs was carried out by making use of the photochemistry of the BP groups, the photochemically produced triplet state of which can abstract hydrogen atoms from almost any polymer, thus generating radicals.[30] In general, BP is excited indirectly to the lowest triplet state (π-π^*) by direct absorption into singlet state (π-π^*) upon irradiation with UV light.[31] The BP ketyl radical and an on-chain polymer radical readily recombine to generate a new C–C bond,[32] thereby resulting in cross-linking within the nanofibers (Figure 1 b). UV/Vis spectroscopy was used to monitor the cross-linking with BP. The absorbance around 305 nm is attributed to the π-π^* transition of the BP moieties in the nanofiber web. The absorbance at 305 nm decreased and almost disappeared after 30 min irradiation with UV light (see Figure S4 in the Supporting Information).

Figure 2 a shows the changes in the surface size of the BP2 cross-linked nanofiber web in response to alternations of temperature between 10 and 37 °C. When dissolved in PBS and heated to 37 °C, the web underwent a drastic shrinking because of a conformational change of the copolymer. The cross-linked nanofibers had an LCST of approximately 18 °C (see Figure S5 in the Supporting Information). The temperature was then alternated below and above the LCST and, correspondingly, the web first swelled, and then shrank. Interestingly, the web did not return to the original size when the temperature was lowered below the LCST. It is plausible that the porosity of the nanofiber web gradually decreased during the heating and cooling cycles, thereby reducing the ability of water to hydrate the entire surface area of the web.

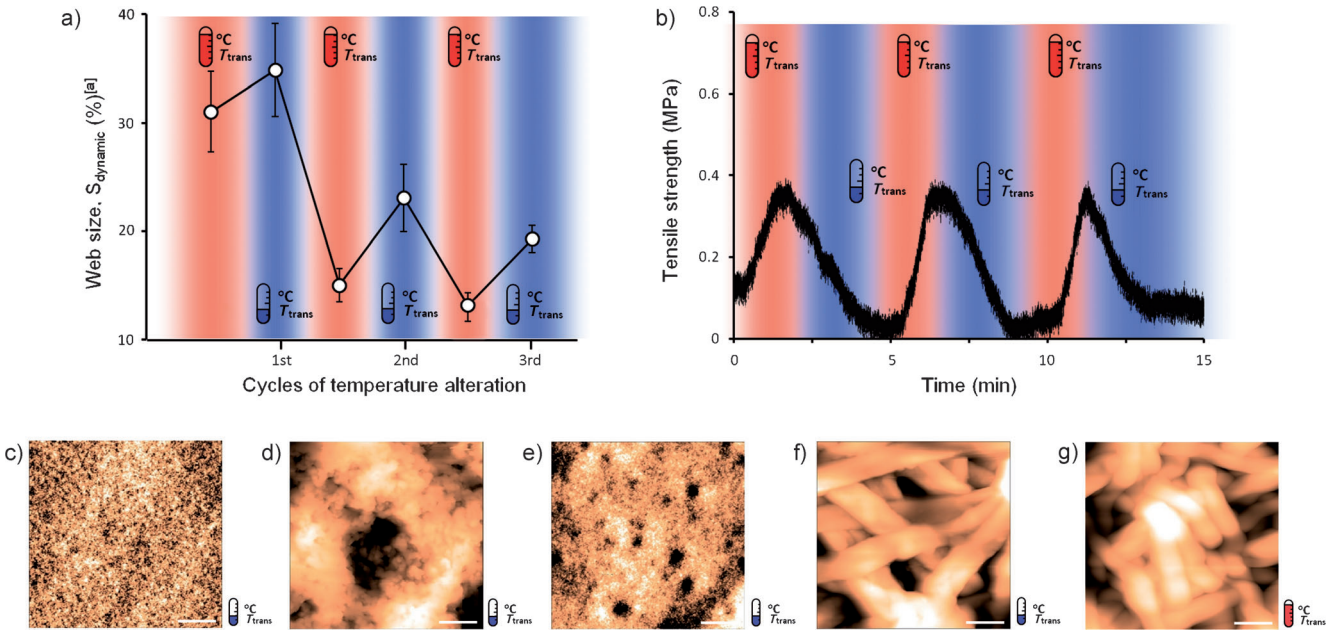

Figure 2. Temperature-dependent changes in the web size (a) and tensile strength (b) of a cross-linked BP2 nanofiber web in response to temperature alternations between 10 and 37 °C. AFM images of non-cross-linked BP1 (c), cross-linked BP1 (d), non-cross-linked BP2 (e), cross-linked BP2 (f) at 10 °C, and cross-linked BP2 (g) at 37 °C (scale bar: 2 μm). [a] $S_{dynamic} = S_T/S_{Dry} \times 100$ (%), where S_T = web size at T (°C), S_{Dry} = web size at dry state.

The tensile strength of the cross-linked nanofiber web was also measured by using a tensile tester housed within a temperature-controlled chamber. The web was fixed with a tensile strength of approximately 500 kPa and then PBS at 37 °C was sprayed over the sample. After 5 min of equilibration, the temperature within the chamber was alternated between 10 and 37 °C, and the changes in the tensile strength were measured continuously while keeping the sample size constant. The tensile strength was found to change reversibly in response to temperature (Figure 2b). Of particular interest is that the changes in the tensile strength during in each cycle were almost constant (ca. 400 kPa). The morphology of the nanofiber web above and below the LCST was also observed by atomic force microscopy (AFM). Figure 2c–g shows the morphologies of BP1 and BP2 nanofibers at 10 and 37 °C. No fibrous structure can be seen for non-cross-linked BP1 and BP2 nanofiber webs at 10 °C because they unraveled and dispersed in an aqueous medium below the LCST (Figure 2c,e). The same result was obtained for the BP1 nanofiber web even after irradiation with UV light (Figure 2d). Fibrous structures, on the other hand, are clearly observed for the cross-linked BP2 nanofiber web both below and above the LCST, although the nanofiber webs shrunk above the LCST (Figure 2f,g). The fiber sizes were larger than those determined from the SEM images because the AFM images were recorded under wet conditions. On the basis of these results, BP2 was selected for further study.

The cell wrapping, encapsulation, and releasing capability of the nanofiber webs were evaluated by incubating cells on the webs. 100 μL of a cell culture medium containing 3.0×10^4 normal human dermal fibroblasts (NHDFs) were dropped on 2.2 cm diameter cross-linked BP2 nanofiber webs at 37 °C. The web immediately started to fold up and wrap around the droplet (Figure 3a). The folding of the web was very fast and was completed after 30 s. After 10 min at 37 °C, the web was transferred to a refrigerator at 4 °C and allowed to swell for another 10 min. The web transformed into a transparent, hydrogel-like morphology (Figure 3b). However, the fibrous structure was maintained (see Figure S6 in the Supporting information). When heated again to 37 °C, the hydrogel-like web shrank and became opaque (Figure 3c). These behaviors were not observed for the non-cross-linked BP2 (see Figure S7 in the Supporting Information). The ability of the nanofiber webs to release the cells was evaluated by collecting released medium from the web on heating from 4 to 37 °C. The medium was then centrifuged to determine the cell numbers. This cycle was repeated three times. The results of the cell-releasing experiments are summarized in Figure 3d. Approximately 70 %, 19 %, and 6 % of the cells were released from the web in the 1st, 2nd, and 3rd cycles of temperature alternation, respectively. In other words, almost all of the cells (> 95 %) seeded on the web were released after three temperature cycles, whereas only negligible amounts of cells were released during the swelling process from 37 to 4 °C.

The cross-linked BP2 nanofiber web undergoes a volume phase transition from a hydrophilic swollen state to a hydrophobic collapsed state when heated to 37 °C. As a consequence, cells are considered to be squeezed out from the web, which may negatively affect cell viability and membrane structure. Therefore, we investigated the viability of the NHDFs released from the nanofiber web. A live/dead assay of the cells released from the web showed that almost all the cells were alive (Figure 3e). An MTT (3-(4,5-dimethylthiazol-2-yl)-2,5-diphenyltetrazolium bromide) assay was also per-

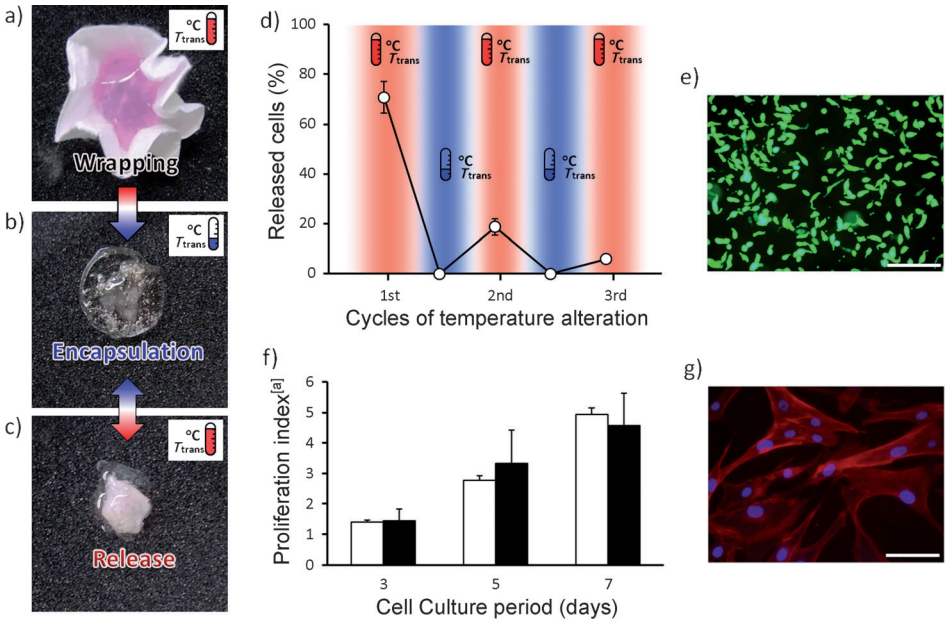

Figure 3. a–c) Wrapping, encapsulation, and release of cells by using the photo-cross-linked BP2 nanofiber web. The droplet of cells is wrapped up at 37 °C (a) and stably encapsulated inside the web, which transforms into a hydrogel-like morphology at 4 °C (b). Upon heating the web again at 37 °C, it shrinks rapidly and releases the entrapped cells (c). d) The percentage of released cells from the web during the heating/cooling processes between 4 and 37 °C. This process was repeated for 3 cycles. e) A live/dead assay was performed to determine the viability of the released cells from the webs (green: live cells, red: dead cells, scale bar: 200 μm). f) An MTT assay illustrates the proliferation potential of the released cells after the 3rd cycle (open bar: cells cultured on TCPS, closed bar: released cells from NF webs). g) Fluorescence images demonstrating the viability of released cells in the 3rd cycle by actin staining with rhodamine-phalloidin (red) and DAPI (blue) after cultivation for 3 days at 37 °C (scale bar: 100 μm). [a] Proliferation index = $N_D/N_{D=1}$, where N_D = cell number on day D, $N_{D=1}$ = cell number on day 1).

formed to determine whether the releasing process adversely affects the health and proliferation of the NHDFs. The released cells were reseeded on tissue culture polystyrene (TCPS) dishes and proliferation was observed. The proliferation index of the released cells in the 1st cycle was not statistically different from the control population (Figure 3 f), thus indicating that the temperature alternations are not acutely toxic to the cells and do not affect the cell proliferation. Furthermore, the viability of the released cells was demonstrated by actin and nuclei staining with rhodamine-phalloidin and 4-6-diamidino-2-phenylindole (DAPI) after cultivation on TCPS. The released cells demonstrated a well-defined cytoskeleton (Figure 3 g). Since the proposed system does not require any reaction/degradation during cell capture/release processes, which are known to be toxic to cells, the smart nanofiber web provides a facile and biologically friendly platform for cell encapsulation and release, especially for therapeutic cell delivery or cell manipulation.

In conclusion, this study describes a novel approach for encapsulating and releasing cells using a smart nanofiber web with dynamically and reversibly tunable web properties without using any cross-linking/degradation processes. The smart web was fabricated by an electrospinning method with a newly synthesized photo-cross-linkable temperature-responsive polymer. By photo-cross-linking, the web showed the ability to trigger "on" or "off" web properties in response to external changes in temperature. By using external signals, we also demonstrated cell capture, encapsulation, and release. The released cells show excellent viability and proliferation behavior. This study extends the capture and release methods to a variety of bioactive compounds,[33] the activity of which can be controlled by switching their accessibility to the environment. Further functionalization of the nanofibers could also be used for the immobilization of peptides or antibodies, which are highly promising for separation, purification, preservation, and the delivery of the target molecules and cells.

Received: May 28, 2012
Published online: September 18, 2012

Keywords: electrospinning · nanofibers · nanostructures · photochemistry · polymers

[1] H.-W. Liang, L. Wang, P.-Y. Chen, H.-T. Lin, L.-F. Chen, D. He, S.-H. Yu, *Adv. Mater.* **2010**, *22*, 4691 – 4695.
[2] Y. Long, H. Chen, Y. Yang, H. Wang, Y. Yang, N. Li, K. Li, J. Pei, F. Liu, *Macromolecules* **2009**, *42*, 6501 – 6509.
[3] Q. Wu, Y. Xu, Z. Yao, A. Liu, G. Shi, *ACS Nano* **2010**, *4*, 1963 – 1970.
[4] S. Soukasene, D. J. Toft, T. J. Moyer, H. Lu, H.-K. Lee, S. M. Standley, V. L. Cryns, S. I. Stupp, *ACS Nano* **2011**, *5*, 9113 – 9121.
[5] a) F. Di Benedetto, E. Mele, A. Camposeo, A. Athanassiou, R. Cingolani, D. Pisignano, *Adv. Mater.* **2008**, *20*, 314 – 318; b) H. Okuzaki, K. Kobayashi, H. Yan, *Macromolecules* **2009**, *42*, 5916 – 5918.
[6] a) H. Okuzaki, K. Kobayashi, H. Yan, *Synth. Met.* **2009**, *159*, 2273 – 2276; b) G. D. Fu, L. Q. Xu, F. Yao, K. Zhang, X. F. Wang, M. F. Zhu, S. Z. Nie, *ACS Appl. Mater. Interfaces* **2009**, *1*, 239 – 243.
[7] S. Ramakrishna, K. Fujihara, W.-E. Teo, T. Yong, Z. Ma, R. Ramaseshan, *Mater. Today* **2006**, *9*, 40 – 50.
[8] A. L. Yarin, W. Kataphinan, D. H. Reneker, *J. Appl. Phys.* **2005**, *98*, 064501.
[9] R. Sen, B. Zhao, D. Perea, M. E. Itkis, H. Hu, J. Love, E. Bekyarova, R. C. Haddon, *Nano Lett.* **2004**, *4*, 459 – 464.
[10] D. Li, Y. Xia, *Nano Lett.* **2004**, *4*, 933 – 938.
[11] B. J. Kim, Y. S. Choi, H. J. Cha, *Angew. Chem.* **2012**, *124*, 699 – 702; *Angew. Chem. Int. Ed.* **2012**, *51*, 675 – 678.
[12] a) W. He, Z. W. Ma, T. Yong, W. E. Teo, S. Ramakrishna, *Biomaterials* **2005**, *26*, 7606 – 7615; b) S. Ko, J. Jang, *Biomacromolecules* **2007**, *8*, 1400 – 1403.
[13] T. J. Sill, H. A. von Recum, *Biomaterials* **2008**, *29*, 1989 – 2006.

[14] C. K. Hashi, Y. Zhu, G.-Y. Yang, W. L. Young, B. S. Hsiao, K. Wang, B. Chu, S. Li, *Proc. Natl. Acad. Sci. USA* **2007**, *104*, 11915 – 11920.
[15] K. S. Rho, L. Jeong, G. Lee, B.-M. Seo, Y. J. Park, S.-D. Hong, S. Roh, J. J. Cho, W. H. Park, B.-M. Min, *Biomaterials* **2006**, *27*, 1452 – 1461.
[16] a) Z. Ding, R. B. Fong, C. J. Long, P. S. Stayton, A. S. Hoffman, *Nature* **2001**, *411*, 59 – 62; b) T. Miyata, N. Asami, T. Uragami, *Nature* **1999**, *399*, 766 – 769; c) M. Ebara, J. M. Hoffman, A. S. Hoffman, P. S. Stayton, *Lab Chip* **2006**, *6*, 843 – 848.
[17] a) K. Nishida, M. Yamato, Y. Hayashida, K. Watanabe, K. Yamamoto, E. Adachi, S. Nagai, A. Kikuchi, N. Maeda, H, Watanabe, T. Okano, Y. Tano, *N. Engl. J. Med.* **2004**, *565*, 6 – 10; b) M. Ebara, K. Uto, N. Idota, J. M. Hoffman, T. Aoyagi, *Adv. Mater.* **2012**, *24*, 273 – 278; c) M. Ebara, M. Yamato, T. Aoyagi, A. Kikuchi, K. Sakai, T. Okano, *Adv. Mater.* **2008**, *20*, 3034 – 3038.
[18] a) A. Chenite, C. Chaput, D. Wang, C. Combes, M. D. Buschmann, C. D. Hoemann, J. C. Leroux, B. L. Atkinson, F. Binette, A. Selmani, *Biomaterials* **2000**, *21*, 2155 – 2161; b) K. Kuwahara, Z. Yang, G. C. Slack, M. E. Nimni, B. Han, *Tissue Eng. Part C* **2010**, *16*, 609 – 618.
[19] a) J. L. Drury, D. J. Mooney, *Biomaterials* **2003**, *24*, 4337 – 4351; b) C.-C. Lin, K. S. Anseth, *Pharm. Res.* **2009**, *26*, 631 – 643.
[20] a) G. D. Nicodemus, S. J. Bryant, *Tissue Eng. Part B* **2008**, *14*, 149 – 165; b) C. G. Williams, A. N. Malik, T. K. Kim, P. N. Manson, J. H. Elisseeff, *Biomaterials* **2005**, *26*, 1211 – 1218.
[21] C. N. Salinas, B. B. Cole, A. M. Kasko, K. S. Anseth, *Tissue Eng.* **2007**, *13*, 1025 – 1034.
[22] S. Prakash, H. S. Lin, *Trends Biomater. Artif. Organs* **2004**, *18*, 24 – 35.
[23] a) R. Yoshida, K. Uchida, Y. Kaneko, K. Sakai, A. Kikuchi, Y. Sakurai, T. Okano, *Nature* **1995**, *374*, 240 – 242; b) A. Suzuki, T. Tanaka, *Nature* **1990**, *346*, 345 – 347; c) M. Heskins, J. E. Guillet, *J. Macromol. Sci. Pure Appl. Chem.* **1968**, *2*, 1441 – 1455.
[24] D. N. Rockwood, D. B. Chase, R. E. Akins, Jr., J. F. Rabolt, *Polymer* **2008**, *49*, 4025 – 4032.
[25] G. Chen, A. S. Hoffman, *Nature* **1995**, *373*, 49 – 52.
[26] a) T. Aoyagi, M. Ebara, K. Sakai, Y. Sakurai, T. Okano, *J. Biomater. Sci. Polym. Ed.* **2000**, *11*, 101 – 110; b) M. Ebara, T. Aoyagi, K. Sakai, T. Okano, *Macromolecules* **2000**, *33*, 8312 – 8316; c) P. Techawanitchai, M. Ebara, N. Idota, T.-A. Asoh, A. Kikuchi, T. Aoyagi, *Soft Matter* **2012**, *8*, 2844 – 2851.
[27] T. Kanda, K. Yamamoto, T. Aoyagi, *J. Photopolym. Sci. Technol.* **2005**, *18*, 515 – 518.
[28] Z.-M. Huang, Y.-Z. Zhang, M. Kotaki, S. Ramakrishna, *Compos. Sci. Technol.* **2003**, *63*, 2223 – 2253.
[29] P. Gupta, C. Elkins, T. E. Long, G. L. Wilkes, *Polymer* **2005**, *46*, 4799 – 4810.
[30] M. Ebara, J. M. Hoffman, P. S. Stayton, A. S. Hoffman, *Radiat. Phys. Chem.* **2007**, *76*, 1409 – 1413.
[31] G. Dorman, G. D. Prestwich, *Biochemistry* **1994**, *33*, 5661 – 5673.
[32] M.-K. Park, S. Deng, R. C. Advincula, *J. Am. Chem. Soc.* **2004**, *126*, 13723 – 13731.
[33] a) K. Yoshimatsu, B. K. Lesel, Y. Yonamine, J. M. Beierle, Y. Hoshino, K. J. Shea, *Angew. Chem.* **2012**, *124*, 2455 – 2458; *Angew. Chem. Int. Ed.* **2012**, *51*, 2405 – 2408; b) M. B. Dainiak, A. Kumar, I. Y. Galaev, B. Mattiasson, *Proc. Natl. Acad. Sci. USA* **2006**, *103*, 849 – 854.

